

# Phase Structure in Blends of Poly(ethylene glycol) and Poly(styrene-*co*-methacrylic acid)

Isamu Akiba, Yasushi Ohba, and Saburo Akiyama\*

Department of Chemical Science and Technology, Faculty of Technology, Tokyo University of Agriculture and Technology, Koganei, Tokyo 184-8588, Japan

Received June 23, 1998

**ABSTRACT:** Phase structures in blends of poly(ethylene glycol) (PEG) and poly(styrene-*co*-methacrylic acid) (P(S-*co*-MAA)) with several contents of methacrylic acid units are investigated by using both optical microscopy and field emission type scanning electron microscopy (FE-SEM). It is found that phase-separated domains are diminished with increasing MAA content in PEG/P(S-*co*-MAA) blends. Further, in the blends in which the ratio of MAA/–CH<sub>2</sub>CH<sub>2</sub>O– is larger than 0.2 (mol/mol), macroscopic phase structures disappeared despite the presence of two  $T_g$ 's meaning separation into two phases in differential scanning calorimetry (DSC) measurements. In PEG/P(S-*co*-MAA) blends in which MAA/–CH<sub>2</sub>CH<sub>2</sub>OEnDash– > 0.2 (mol/mol), phase-separated structures like interpenetrating networks are found by FE-SEM observations.

## Introduction

It is well-known that polymer mixtures are immiscible due to a high degree of polymerization and positive interaction parameter.<sup>1</sup> Hence, phase behavior of polymer blends is strongly affected by intermolecular associations, for example, hydrogen bonding.<sup>1,2</sup> Introducing a polar group to one component, which is able to associate with another component, would enhance the miscibility of immiscible polymer blends. In addition, it has been predicted that mesomorphic phase structures, such as interpenetrating polymer network (IPN) and microphase separation, are caused despite a macroscopically homogeneous state due to balance of intermolecular association and repulsion.<sup>2–5</sup> These predictions are supported by several experimental results in associating polymer systems.<sup>6–11</sup> Hence, in the associating polymer blends, the appearance of specific phase structures is expected in a macroscopically homogeneous state. In this paper, we focus on the phase-separated structure in associating polymer blends using poly(ethylene glycol) (PEG) and poly(styrene-*co*-methacrylic acid) (P(S-*co*-MAA)).

It has been well-known that the blends of poly(ethylene glycol) and polystyrene (PS) are immiscible in a wide temperature and composition range.<sup>12</sup> Further, it has been also well-known that PEG and poly(methacrylic acid) (PMAA) form a complex due to association between carboxylic acid of PMAA and ether oxygen of PEG.<sup>13,14</sup> In addition, it was found out by Coleman et al. that poly(ethylene-*co*-methacrylic acid) (EMAA)/poly(ethylene oxide) (PEO) blends are miscible in certain composition due to carboxylic acid–ether interaction between EMAA and PEO while polyethylene and PEG are immiscible in a wide temperature and composition range.<sup>15,16</sup> Therefore, the blends of PEG and P(S-*co*-MAA) would have a wider miscible region than PEG/PS blends in the temperature–composition plane. However, if P(S-*co*-MAA) includes a relatively small amount of MAA unit, repulsive forces between PS and PEG sufficiently remain. Therefore, specific phase

**Table 1. Molecular Characteristics of PEG and P(S-*co*-MAA)**

sample	$\overline{M}_w \times 10^{-3}$	$\overline{M}_w/\overline{M}_n$	$T_g/^\circ\text{C}$	$T_m/^\circ\text{C}$
PEG	4.0		–50	48
PS	37.0		105	
P(S- <i>co</i> -MAA) <sub>4.8</sub>	28.0	2.55	110	
P(S- <i>co</i> -MAA) <sub>7.2</sub>	29.5	2.52	119	
P(S- <i>co</i> -MAA) <sub>12</sub>	30.2	2.58	128	
P(S- <i>co</i> -MAA) <sub>18</sub>	30.8	2.55	138	
P(S- <i>co</i> -MAA) <sub>27</sub>	20.8	2.36	145	

structures might be expected to appear in PEG/P(S-*co*-MAA) blends by using P(S-*co*-MAA) with low MAA content due to the balance of associating force between MAA and PEG and repulsive force between PS and PEG. Then, in the present paper, we report on the miscibility and phase structures in the blends of PEG and P(S-*co*-MAA) to reveal the relationship between intermolecular association and the phase-separated associating polymer blends.

## Experiments

**Materials.** Polymers used in this study were poly(ethylene glycol), PEG, and poly(styrene-*co*-methacrylic acid)s, P(S-*co*-MAA)<sub>x</sub>, with MAA contents of 0, 4.8, 7.2, 12, 18, and 27 mol %. PEG sample was purchased from Wako Pure Chemicals Co., Ltd., and P(S-*co*-MAA)<sub>x</sub> samples were kindly supplied from Dainippon Ink Co., Ltd. Here, subscript *x* of P(S-*co*-MAA) denotes mole percentage of MAA units in P(S-*co*-MAA). The molecular characteristics of PEG and P(S-*co*-MAA)<sub>x</sub> were listed in Table 1. In Table 1, the glass transition temperature,  $T_g$ , and melting temperature,  $T_m$ , were determined as the midpoint of transition and the extrapolated onset point of melting peak in DSC thermograms, respectively.

**Preparation of Blend Samples.** Blend samples of PEG and P(S-*co*-MAA) were prepared by solution mixing using 1:1 (v/v) mixture of tetrahydrofuran and chloroform as a solvent. Both polymers weighted in desired blend composition were dissolved in the solvent and mechanically stirred until the solution became transparent. The clear solution were cast onto glass plates and placed at room temperature until most of solvents were evaporated from samples. As-cast film specimens were further dried under reduced pressure at 40 °C for 1 week and at  $T_g + 20$  °C of each P(S-*co*-MAA) for 2 h. Resulting samples were annealed at 160 °C for 2 h in reduced pressure and quenched in liquid N<sub>2</sub> before any measurements. The

\* Corresponding author.

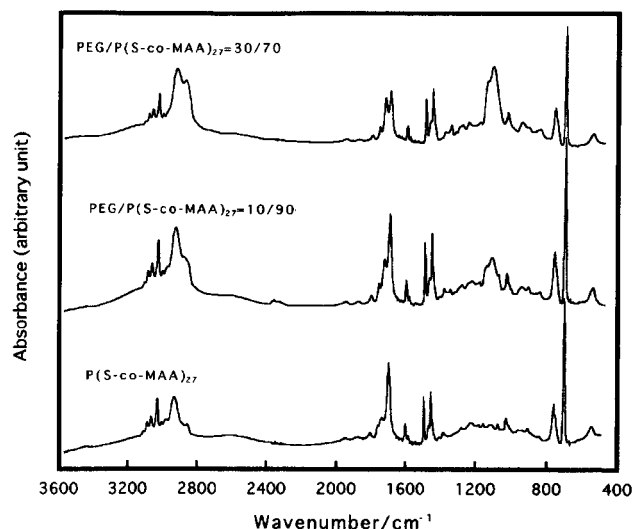


**Figure 1.** Infrared spectra for PEG/P(S-*co*-MAA)<sub>27</sub> blends.

anneal temperature (160 °C) was selected because the temperature situated between  $T_g$  of P(S-*co*-MAA)s and the reactive temperature of dehydration of carboxylic acids.

**Infrared Spectroscopy.** Infrared spectroscopy was performed using a JEOL JIR-WINSPEC35 FT-IR spectrometer at a resolution of 2  $\text{cm}^{-1}$  for thin-film specimens. A minimum of 100 scans were signal averaged. All the FT-IR measurements were taken at room temperature.

**Optical Microscopy.** Film specimens were set between glass plates. For the samples, morphological observations were performed using a Nikon S-Ke optical microscope equipped with a hot stage. All the optical micrographs were taken at 160 °C.

**Scanning Electron Microscopy.** Samples were annealed at 160 °C for 2 h and then quenched and fractured in liquid  $\text{N}_2$ . The fractured surfaces were etched by distilled water for 1 min to remove the PEG-rich phase from the surface and sputtered by tungsten. For these samples, SEM observations were performed by using an Elionix ERA-8000FE, field emission type SEM (FE-SEM).

## Results and Discussion

In PEG/P(S-*co*-MAA) blends, it is expected that association is formed between carboxylic acid in P(S-*co*-MAA) and ether oxygen in PEG.<sup>13–16</sup> FT-IR is one of the powerful tools for the investigation of intermolecular associations in polymer blends.<sup>1</sup> Figure 1 shows the FT-IR spectra for PEG/P(S-*co*-MAA)<sub>27</sub> = 0/100, 10/90, and 30/70 (w/w) blends. In these spectra, remarkable differences of FT-IR spectra between P(S-*co*-MAA)<sub>27</sub> and PEG/P(S-*co*-MAA)<sub>27</sub> blends appear in the absorbance around 1100, 1700, and 2900  $\text{cm}^{-1}$ , which are attributed to the antisymmetric stretching band of ether bond of PEG, the carbonyl stretching band of P(S-*co*-MAA)<sub>27</sub>, and the methylene stretching band, respectively. The peaks around 1100 and 2900  $\text{cm}^{-1}$  changed systematically with changing blend composition. On the other hand, the intensity of one peak around 1700  $\text{cm}^{-1}$  increased with increasing weight fraction of PEG; nevertheless, there is no absorption around 1700  $\text{cm}^{-1}$  in PEG. FT-IR spectra around 1700  $\text{cm}^{-1}$  for PEG/P(S-*co*-MAA)<sub>27</sub> = 0/100, 10/90, and 30/70 (w/w) blends are magnified in Figure 2. The absorbances centered at 1697 and 1725  $\text{cm}^{-1}$  are attributed to the carbonyl stretching band of carboxylic acid dimer and free carbonyl groups, respectively.<sup>15,16</sup> In P(S-*co*-MAA)<sub>27</sub>, the absorbance from the dimer of carboxylic acids is strong because the carboxylic acids are fully dimerized. On the contrary,

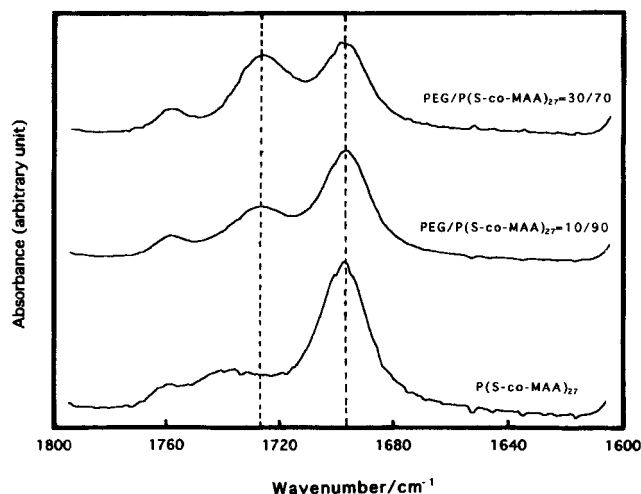


**Figure 2.** Infrared spectra for PEG/P(S-*co*-MAA)<sub>27</sub> blends in the 1700  $\text{cm}^{-1}$  region.

the absorbance from free carbonyl groups clearly appeared in PEG/P(S-*co*-MAA)<sub>27</sub> blends. In addition, the intensity of the absorbance of the free carbonyl become relatively strong against that of the carboxylic acid dimer with increasing PEG contents in PEG/P(S-*co*-MAA)<sub>27</sub> blends. Hence, the amounts of free carbonyl groups of P(S-*co*-MAA)<sub>27</sub> are increasing with increasing blend composition of PEG. This result is similar to the results of Coleman et al.<sup>15–17</sup> The reason free carbonyl groups are formed in PEG/P(S-*co*-MAA) blends is that carboxylic acid dimers are debonded due to the formation of carboxylic acid–ether oxygen interaction between the hydroxyl group in the carboxyl group and PEG.<sup>15–17</sup> Since the PEG/P(S-*co*-MAA) blends are regarded as associating polymer blends, it is of great importance for this system to investigate the phase-separated structures.

Figure 3 shows optical micrographs taken at 160 °C for PEG/PS, PEG/P(S-*co*-MAA)<sub>7.2</sub>, and P(S-*co*-MAA)<sub>27</sub> = 30/70 (w/w) blends. As can be seen in these photographs, large droplets whose diameter was in the range 1–10  $\mu\text{m}$  are observed in the PEG/PS = 30/70 (w/w) blend. On the other hand, the phase-separated structures which are much smaller than that of the PEG/PS blend are found in PEG/P(S-*co*-MAA)<sub>7.2</sub> = 30/70 (w/w) blends. Further, the presence of continuity is recognized in the phase-separated structure in the PEG/P(S-*co*-MAA)<sub>7.2</sub> blend. In addition, phase-separated structures disappear in the PEG/P(S-*co*-MAA)<sub>27</sub> blend. From the results, the sizes of the phase-separated domains of PEG/P(S-*co*-MAA) blends become smaller with increasing MAA contents in P(S-*co*-MAA), and finally the domains are not observed in blends of PEG and P(S-*co*-MAA) with high MAA content by an optical microscope. The same changes of the phase-separated structures are also found by varying the blend composition in PEG/P(S-*co*-MAA) blends. Figure 4 shows optical micrographs taken at 160 °C for PEG/P(S-*co*-MAA)<sub>7.2</sub> and PEG/P(S-*co*-MAA)<sub>12</sub> = 40/60, 30/70, and 20/80 (w/w) blends. The phase-separated structures are observed in PEG/P(S-*co*-MAA)<sub>7.2</sub>  $\geq$  30/70 (w/w) blends. On the contrary, in PEG/P(S-*co*-MAA)<sub>7.2</sub>  $\leq$  20/80 (w/w) blends, the presence of phase-separated structure is not observed by optical microscopy. On the basis of the results in Figures 3 and 4, it is considered that the change in the morphology of PEG/P(S-*co*-MAA) blends is caused by a balance of association between the carboxylic acid and ether

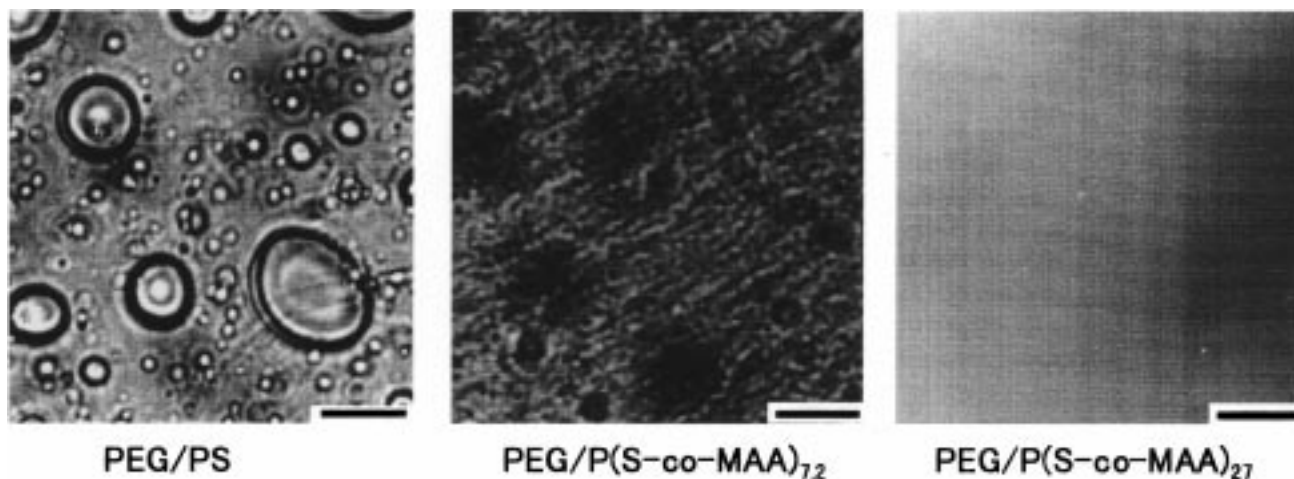


**Figure 3.** Optical micrographs of PEG/P(S-*co*-MAA) = 30/70 (w/w) blends with various MAA contents taken at 160 °C.

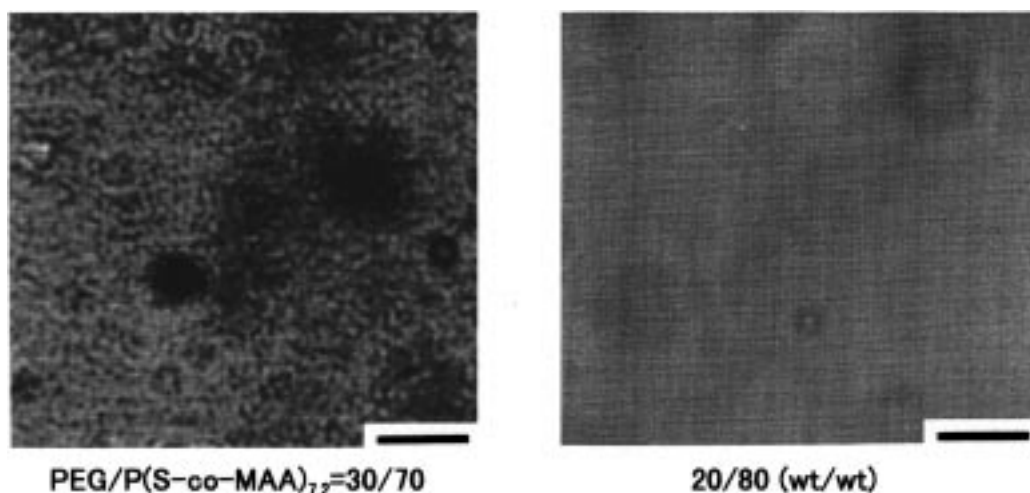


**Figure 4.** Optical micrographs of PEG/P(S-*co*-MAA)<sub>7.2</sub> blends with various blend compositions taken at 160 °C.

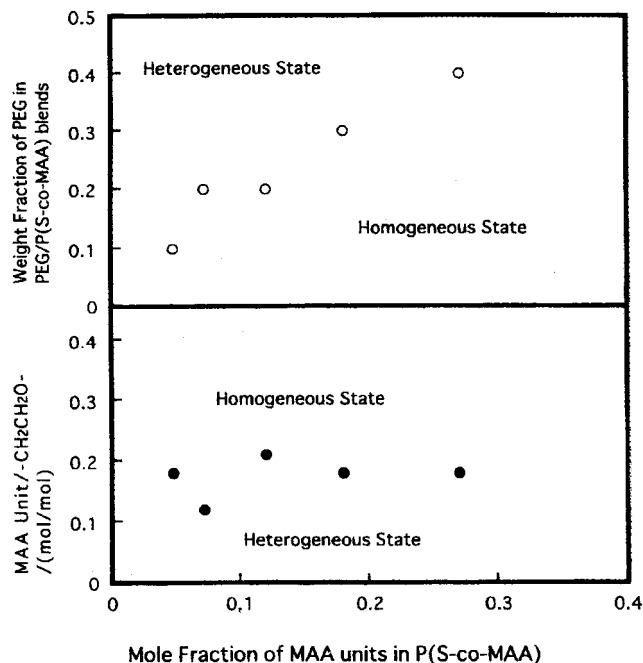
oxygen and repulsion between the styrene unit and PEG. Hence, it is predicted that the boundary at which homogenization occurs is correlated with the amount of MAA unit in PEG/P(S-*co*-MAA) blends.

Figure 5 shows the plots of the boundary between macroscopic phase separation and homogeneous state against MAA contents in P(S-*co*-MAA). In the top figure of Figure 5, mole fractions of PEG at the boundary are plotted against MAA contents in P(S-*co*-MAA). The range of blend composition forming homogeneous mixtures becomes larger with increasing MAA contents in P(S-*co*-MAA). Since the homogeneous states of PEG/P(S-*co*-MAA) blends are enhanced by carboxylic acid-ether interaction between MAA and ether oxygen of PEG, it is considered that there is a relationship between the ratio of MAA/ether oxygen of PEG ( $-\text{CH}_2\text{CH}_2\text{O}-$ ) and the boundary. In the bottom of Figure 5, molar ratios of  $\text{MAA}/-\text{CH}_2\text{CH}_2\text{O}-$  at the boundary are plotted against MAA contents of P(S-*co*-MAA). As can be seen in this figure, the molar ratio of MAA units against ether units are almost constant,  $\text{MAA}/-\text{CH}_2\text{CH}_2\text{O}- \sim 0.2$  (mol/mol), regardless of MAA contents in P(S-*co*-MAA). This value ( $\text{MAA}/-\text{CH}_2\text{CH}_2\text{O}- = 0.2$ ) would suggest a stoichiometric rule in homogenization of PEG/P(S-*co*-MAA) blends, though the value was obtained incidentally. This relationship supports that the homogenization of PEG/P(S-*co*-MAA) blends is caused by the association between the carboxylic acid of P(S-*co*-MAA) and ether oxygen of PEG. That is to say, the

repulsive force between the styrene unit and PEG is dominant when  $\text{MAA}/-\text{CH}_2\text{CH}_2\text{O}- < 0.2$  and the associative force between MAA and ether oxygen is dominant when  $\text{MAA}/-\text{CH}_2\text{CH}_2\text{O}- > 0.2$ . However, it is obscure that PEG/P(S-*co*-MAA) blends are miscible in the homogeneous state. Then, DSC measurements are performed for PEG/P(S-*co*-MAA) blends to examine the miscibility in this system.

Figures 6 and 7 show DSC thermograms of PEG/P(S-*co*-MAA)<sub>7.2</sub> and PEG/P(S-*co*-MAA)<sub>27</sub> blends, respectively. These thermograms are obtained for the samples annealed at 160 °C where the photographs shown in Figures 3 and 4 are taken. In PEG-rich blends, since melting peaks of PEG are detected but  $T_g$ 's of both PEG and P(S-*co*-MAA) are not recognized, miscibility of the blends is not estimated. On the other hand, in P(S-*co*-MAA)-rich blends, two  $T_g$ 's arisen from PEG and P(S-*co*-MAA) are clearly detected despite the homogeneity of PEG/P(S-*co*-MAA) blends. Therefore, it is expected that microscopic heterogeneity is present in PEG/P(S-*co*-MAA) blends in the P(S-*co*-MAA)-rich region. Then, FE-SEM observations are carried out for these blends.

Figure 8 shows FE-SEM micrographs for P(S-*co*-MAA)<sub>27</sub> = 10/90 (w/w) blends. These photographs are taken for the samples annealed at 160 °C and quenched in liquid N<sub>2</sub>. Since the fractured surfaces of the samples are etched by distilled water, bright and dark parts correspond to the P(S-*co*-MAA)-rich and PEG-rich phase, respectively. As can be seen in these photographs, the



**Figure 5.** Plots of boundary between macroscopically homogeneous and heterogeneous state at 160 °C against MAA contents in P(S-co-MAA).

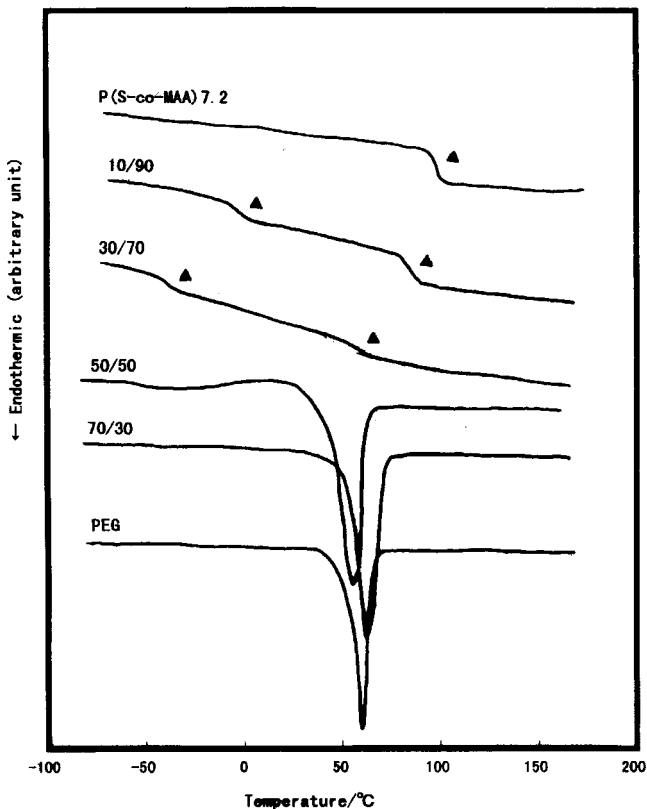


**Figure 6.** DSC thermograms of PEG/P(S-co-MAA)<sub>7.2</sub> blends annealed at 160 °C for 2 h and quenched in liquid N<sub>2</sub>.

phase-separated structures like interpenetrating networks are observed in P(S-co-MAA)<sub>27</sub> = 10/90 (w/w) blends. In other compositions of PEG/P(S-co-MAA) blends which are located in the homogeneous region in the bottom of Figure 5, such structures are also found. Hence, it is expected that the specific structures are induced by the carboxylic acid-ether interaction. However, if the effective interaction were only carboxylic

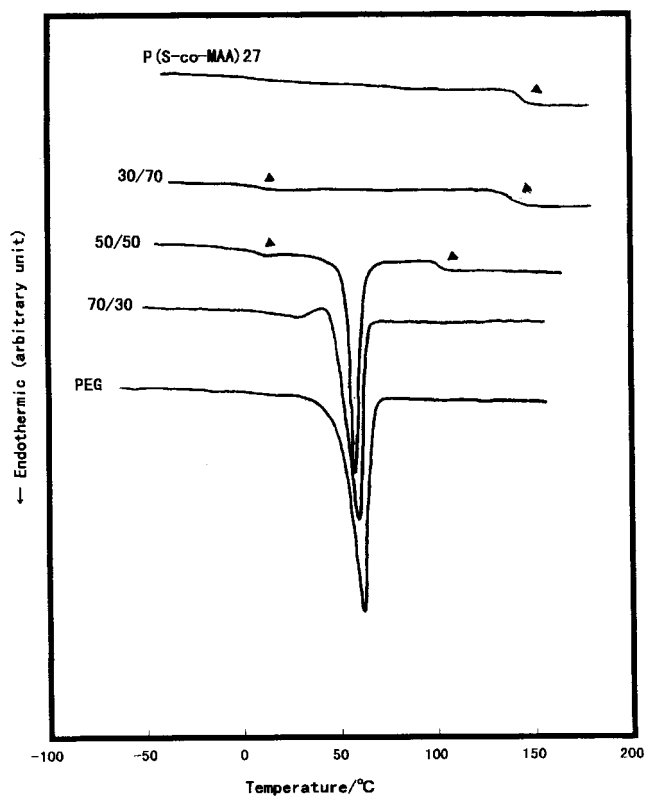


**Figure 7.** DSC thermograms of PEG/P(S-co-MAA)<sub>27</sub> blends annealed at 160 °C for 2 h and quenched in liquid N<sub>2</sub>.

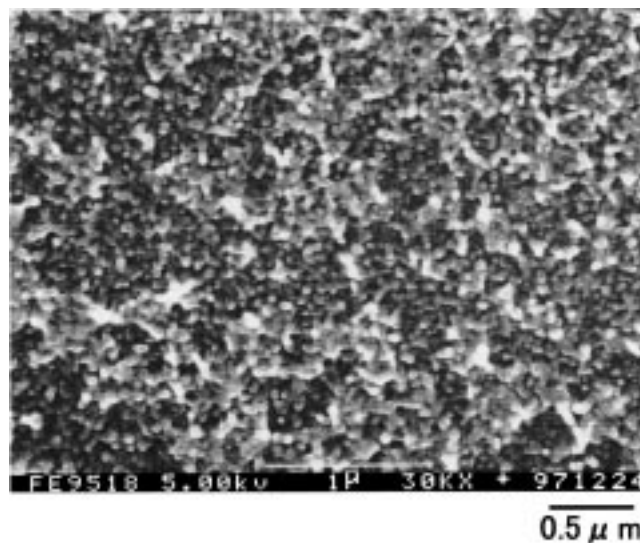


**Figure 8.** SEM micrographs of PEG/P(S-co-MAA)<sub>27</sub> = 10/90 (w/w) blends. Samples were annealed at 160 °C and then quenched and fractured in liquid N<sub>2</sub>. The fractured surfaces were etched by distilled water.

acid-ether oxygen association, there would not be presence of microscopic heterogeneity in this system. Repulsive forces which direct the blends to macroscopic phase separation play an important role in the formation of the structure as well as the attractive force. Therefore, it is considered that the microscopic heterogeneity is induced by the balance between the associating force of carboxylic acid-ether oxygen and the repulsive force of PS and PEG. Since there are relatively long PS chains in P(S-co-MAA) due to low MAA content in P(S-co-MAA) (<27mol %), the repulsive force between PS and PEG still remained in PEG/P(S-co-MAA) blends.

Therefore, microscopic heterogeneity appears by association between carboxylic acid and ether oxygen and repulsion between PS and PEG. If MAA content in P(S-co-MAA) were much higher, microscopic heterogeneity would not appear due to the weak repulsive force. From the results of this study, it is pointed out that the phase-separated structures in associating polymer blends are formed by the balance of the associating forces and the forces directing macroscopic phase separation.

### Concluding Remarks

The phase-separated structures in PEG/P(S-co-MAA) blends are investigated relating to association between the PEG and MAA unit in P(S-co-MAA). These blends are phase-separated regardless of MAA contents. However, in the ratio of MAA/—CH<sub>2</sub>CH<sub>2</sub>O—, which is larger than 0.2 (mol/mol), macroscopic phase-separated structures disappear; nevertheless, the blends have two *T<sub>g</sub>*'s in DSC measurements. In this region, spherical domains of about 50 nm diameter are found in morphological observations using FE-SEM. The minute structures are formed due to the balance of the associating force between the MAA unit and ether oxygen and the repulsive force between PS and PEG. Hence, it is concluded that phase-separated structure in an immiscible polymer blend can be controlled by the adjustment of the balance between attractive force and repulsive force.

**Acknowledgment.** The author expressed his gratitude to Mr. Y. Taguchi of Elionix Co. Ltd. for his helpful support in FE-SEM observations.

### References and Notes

- (1) Coleman, M. M.; Graf, J. F.; Painter, P. C. *Specific Interaction and the Miscibility of Polymer Blends*; Technomic: Lancaster, 1991.
- (2) Hobbie, E. K.; Han, C. C. *J. Chem. Phys.* **1996**, *105*, 738.
- (3) Tanaka, F. *Adv. Colloid Interface Sci.* **1996**, *63*, 23.
- (4) Tanaka, F.; Ishida, M.; Matsuyama, A. *Macromolecules* **1991**, *24*, 5582.
- (5) Tanaka, F.; Ishida, M. *Physica A* **1994**, *204*, 660.
- (6) Cao, Y.; Smith, P. *Polymer* **1993**, *34*, 3139.
- (7) Ruokolainen, J.; ten Brinke, G.; Ikkala, O.; Torkkeli, M.; Serima, R. *Macromolecules* **1996**, *29*, 3409.
- (8) Ikkala, O.; Ruokolainen, J.; ten Brinke, G.; Torkkeli, M.; Serima, R. *Macromolecules* **1995**, *28*, 7088.
- (9) Bazuin, C. G.; Brandy, F. A. *Chem. Mater.* **1992**, *4*, 970.
- (10) Bazuin, C. G.; Plante, M.; Varshney, S. K. *Macromolecules* **1997**, *30*, 2618.
- (11) Tal'roze, R. V.; Kuptsov, S. A.; Sycheva, T. I.; Benzborodov, V. S.; Plate, N. A. *Macromolecules* **1995**, *28*, 8689.
- (12) Utracki, L. A. *Polymer Alloys and Blends*; Carl Hanser: Germany, 1990.
- (13) Tsuchida, E.; Osada, Y.; Ohno, H. *J. Macromol. Sci.-Phys.* **1980**, *B17*, 683.
- (14) Osada, Y. *J. Polym. Sci., Polym. Chem. Ed.* **1979**, *14*, 129.
- (15) Coleman, M. M.; Lee, J. Y.; Serman, J.; Wang, Z.; Painter, P. C. *Polymer* **1989**, *30*, 1298.
- (16) Lee, J. Y.; Painter, P. C.; Coleman, M. M. *Macromolecules* **1988**, *29*, 1659.
- (17) Painter, P. C.; Park, Y.; Coleman, M. M. *Macromolecules* **1989**, *22*, 570.

MA980981O